AIP | Journal of Renewable and Sustainable Energy

Wave energy conversion of oscillating water column devices including air compressibility

Wanan Sheng and Anthony Lewis

Citation: Journal of Renewable and Sustainable Energy **8**, 054501 (2016); doi: 10.1063/1.4963237
View online: http://dx.doi.org/10.1063/1.4963237
View Table of Contents: http://scitation.aip.org/content/aip/journal/jrse/8/5?ver=pdfcov
Published by the AIP Publishing

Wave energy conversion of oscillating water column devices including air compressibility

Wanan Sheng[a] and Anthony Lewis
University College Cork, Cork, Ireland

(Received 28 October 2015; accepted 9 September 2016; published online 23 September 2016)

This paper presents an investigation on air compressibility in the air chamber and its effects on the power conversion of oscillating water column (OWC) devices. As it is well known that for practical OWC plants, their air chambers may be large enough for accommodating significant air compressibility, the "spring effect," an effect that is frequently and simply regarded to store and release energy during the reciprocating process of a wave cycle. Its insight effects on the device's performance and power conversion, however, have not been studied in detail. This research will investigate the phenomena with a special focus on the effects of air compressibility on wave energy conversion. Air compressibility itself is a complicated nonlinear process in nature, but it can be linearised for numerical simulations under certain assumptions for frequency domain analysis. In this research work, air compressibility in the OWC devices is first linearised and further coupled with the hydrodynamics of the OWC. It is able to show mathematically that in frequency-domain, air compressibility can increase the spring coefficients of both the water body motion and the device motion (if it is a floating device), and enhance the coupling effects between the water body and the structure. Corresponding to these changes, the OWC performance, the capture power, and the optimised Power Take-off (PTO) damping coefficient in the wave energy conversion can be all modified due to air compressibility. To validate the frequency-domain results and understand the problems better, the more accurate time-domain simulations with fewer assumptions have been used for comparison. It is shown that air compressibility may significantly change the dynamic responses and the capacity of converting wave energy of the OWC devices if the air chamber is very large. *Published by AIP Publishing*. [http://dx.doi.org/10.1063/1.4963237]

I. INTRODUCTION

Wave energy is known to have massive resources around the world: the global gross resource is about 3.7 TW,[1] and thus it is often envisaged that wave energy is able to significantly contribute energy mix and blue economy. In Europe, it is expected to supply some 10% of the European electricity needs—about half of today's total installed renewable generation if the technologies are matured (the combined wave and tidal energy in Europe would be 100 GW capacity by 2050[2]). Great efforts on extracting wave energy from seas have been for a few decades, and historically more than 1000 different devices with different wave energy conversion principles have been invented[3] (according to Falcao,[4] the majorities of wave energy converters can be classified into three main types, namely, oscillating water column (OWC), oscillating body, and overtopping wave energy converters). However, only a few of the concepts and devices have been or are being developed[5–13] and some of them have even generated wave power to grid.[7,12] So far, there is no consensus among the wave energy technologies,[2] but one significant feature and challenge is the large forces provided by the low velocity waves. This particular feature is simply opposite to that of the conventional energy technologies in which a high speed (or rotational speed) and a low force/torque are used for power conversion, and thus

[a]Email: w.sheng@ucc.ie

applies the challenges on the power performance (normally with low energy conversion efficiency) and reliability (low reliability in wave energy production means high costs for operation and maintenance and for the unplanned interventions and downtime).

OWCs have been regarded as one of the most promising and developed wave energy converters, and probably the most practical and reliable wave energy converters due to their unique wave energy conversion principle. Instead of utilising the motion of the device structure(s) directly for power conversion like other wave energy converters, OWCs employ the air flow which is driven by the internal water surface (IWS) motion in the OWC devices. In power conversion in the OWC devices, the air flow is normally accelerated by many times, so for driving the air turbine Power Take-offs (PTOs) in high rotational speeds.[14] This allows a low torque acting on the PTOs and thus a high reliability of the OWC PTO for a long-term wave energy production.[15,16] The good examples are those practical wave power plants which have been developed and generated power to the grid, and these practices have proven that the OWC plants have very high reliability in long-term wave power generation. It is reported that the LIMPET OWC plant has generated electricity to the grid for more than 60 000 h in a period of about 10 years,[7] whilst a more recent development is the Mutriku OWC wave energy plant in Spain.[12] A recent review on the development of the OWC devices and air turbines has been given by Falcao and Henriques.[17]

To understand and improve their power performance by the OWC devices, numerical methods have been developed and employed. Earlier theoretical work on the hydrodynamic performance of some simple OWCs has shown that the OWC devices could have a high primary wave energy conversion efficiency.[18–20] Similarly, the boundary element methods (and the relevant commercial software, such as WAMIT, ANSYS AQWA etc.) are more popular for any complexity of the geometries of the OWC devices.[15,21–24] For air compressibility in the OWC devices, some investigations have been carried out.[15,16,23,25–29] Sarmento *et al.*[26] first put forward a formula for air compressibility under the assumption of a large volume of the air chamber (compare to the air volume changes). This equation has been widely accepted and used by other researchers.[28,30] Recently, Sheng *et al.*[15,16,27] have developed the dynamic equations for fully coupling the thermodynamics for accommodating air compressibility and the hydrodynamics of the OWC devices. However, the effects of air compressibility have not been systematically studied on how the device performance and power conversion capacity can be modified.

The importance of studying air compressibility using numerical modelling is because air compressibility is not scalable using the conventional Froude similarity, as shown by Weber,[31] Sheng *et al.*,[32] and Falcao and Henriques.[33] For modelling air compressibility, the volume of the air chamber must be scaled using the square of the scale ratio, rather than that of the cube of the scale ratio as required by the Froude similarity. This means that the physical scale model may need a much larger air chamber. For instance, for a 1:50 scale OWC model, the air volume would be required to be 50 times larger for that required by Froude similitude. Practically, it is very difficult and may be impossible for the floating OWCs.

In this research, the issues with air compressibility in the OWC device will be studied in detail by further formulating air compressibility and coupling it into the hydrodynamic equation of the OWC device in frequency domain. By employing the simplified and linearised PTO airflow equation proposed by Sarmento *et al.*,[26] and including a linear air turbine PTO, the full dynamic equation for accommodating air compressibility and hydrodynamics for the OWC devices can be established in frequency domain. The analyses have then been made in examining the effects of air compressibility on the OWC performances, including both the motion responses and power conversion. Also, to validate the frequency-domain, analysed comparisons have been made for the results of time domain analyses, for which fewer assumptions have been adopted and thus more accurate modelling is expected.

The arrangement of the context is as follows. In Section II, the frequency domain formulations are derived for the dynamics with air compressibility whilst in Section III a short introduction of the formulas of time domain analysis is given; in Section IV the power conversion in irregular waves is formulated; Section V provides the examples and analyses and Section VI, an analysis on the fixed OWC device. In Section VII, conclusions of the research work are given.

II. DYNAMICS OF POWER CONVERSION

Following Sheng *et al.*,[15] a two-body system for the OWCs will be used. In the convention, the first rigid body may be the device itself and the second rigid body is an imaginary thin piston at the internal free surface which replaces part of the water body in the water column.

A. Air flow

The air mass in the air chamber can be calculated as

$$m = \rho V, \tag{1}$$

where m is the air mass in the air chamber; ρ the air density in the air chamber, and V is the air volume of the air chamber.

Differentiating the air mass with regard to time, we have the mass flowrate passing the PTO as

$$\frac{dm}{dt} = \rho \frac{dV}{dt} + V \frac{d\rho}{dt}. \tag{2}$$

It should be noted that the negative mass flowrate means an exhalation of the airflow since the mass is reduced in the air chamber in this case.

Following Sarmento *et al.*[26] and Sheng *et al.*,[27] the air in the chamber can be regarded as isentropic, i.e.,

$$\frac{p_0 + p}{\rho^{\gamma}} = \frac{p_0}{\rho_0^{\gamma}}, \tag{3}$$

where ρ is the air density in the air chamber; ρ_0 is the atmospheric air density; p is the chamber gauge pressure; p_0 is the atmospheric pressure; and γ is the air specific heat ratio (i.e., $\gamma = 1.4$).

Considering the air chamber gauge pressure is normally much smaller than the atmospheric pressure (maximal gauge pressure in the air chamber is probably about 10^4 Pa vs. the atmospheric pressure, 10^5 Pa), so we can have a simplified/linearised density expression as

$$\rho = \rho_0 \left(1 + \frac{p}{\gamma p_0}\right), \tag{4}$$

differentiating (4) with regard to time yields

$$\frac{d\rho}{dt} = \frac{\rho_0}{\gamma p_0} \frac{dp}{dt}. \tag{5}$$

Now the air flowrate through the PTO is defined as

$$q_{pto} = -\frac{1}{\rho_0} \frac{dm}{dt}, \tag{6}$$

where the negative sign means that an exhalation of air from the air chamber produces a positive flowrate through the PTO.

The air flowrate driven by the internal water surface (IWS) in the OWC device is given as

$$q_w = -\frac{dV}{dt}. \tag{7}$$

The negative sign in (7) ensures an equal flowrate driven by the internal water surface and through the PTO if the air compressibility is not included.

Substituting (4)–(7) into (2), we have

$$q_{pto} = \left(1 + \frac{p}{\gamma p_0}\right) q_w - \frac{V}{\gamma p_0}\frac{dp}{dt}. \tag{8}$$

Sarmento *et al.*[26] provided a simplified and linearised form of the equation as

$$q_{pto} = q_w - \frac{V_0}{\gamma p_0}\frac{dp}{dt}. \tag{9}$$

Obviously, this formula assumes the air chamber is large enough so that the internal water surface motion may not change too much of the air volume; and the air chamber pressure is significantly less than the atmospheric pressure. It will be shown that these assumptions may be justified for the practical OWC devices/plants.

B. Power conversion with a linear PTO

For the purpose of analysis, we consider a linear air turbine PTO, for instance, the Wells turbine, due to its roughly linear relation between the flow rate and the pressure across the turbine. For a linear turbine, the pressure is calculated as

$$p = k_1 q_{pto}, \tag{10}$$

where k_1 is the damping coefficient of the turbine and q_{pto} is the complex amplitude of the volume flow rate through the air turbine PTO.

Equation (9) can be written in the frequency domain as

$$q_{pto} = q_w - i\omega \frac{V_0}{\gamma p_0} p. \tag{11}$$

Combining (10) and (11) yields

$$p = k_1 q_w \left(1 - i\omega k_1 \frac{V_0}{\gamma p_0}\right) \Big/ C_1, \tag{12}$$

and the flowrate through the PTO is given by

$$q_{pto} = q_w \left(1 - i\omega k_1 \frac{V_0}{\gamma p_0}\right) \Big/ C_1, \tag{13}$$

with

$$C_1 = 1 + \left(k_1 \omega \frac{V_0}{\gamma p_0}\right)^2. \tag{14}$$

The average power conversion can be given by

$$\bar{P} = \frac{1}{2}\mathrm{Re}\left(p \times q_{pto}^*\right) = \frac{1}{2} k_1 |q_w|^2 / C_1. \tag{15}$$

C. Floating OWC devices with air compressibility

For the floating OWCs, especially the cylindrical OWCs, the internal water surface motion for power conversion can be considered as the result of the heave motions of the structure ("body 1,"

motion mode index: 1–6) and the "imaginary piston" ("body 2," motion mode index: 7–12). For the cylindrical OWC, the main motions for wave power conversion are the heave motions of the structure and the water body. Therefore, the dynamic equation can be expressed as

$$\begin{cases} [i\omega Q_{33} + b_{33} + B_{33}]v_3 + [i\omega Q_{39} + b_{39}]v_9 = f_3 + A_0 p \\ [i\omega Q_{93} + b_{93}]v_3 + [i\omega Q_{99} + b_{99} + B_{99}]v_9 = f_9 - A_0 p, \end{cases} \tag{16}$$

with

$$\begin{cases} Q_{33} = m_{33} + a_{33} - \dfrac{c_{33}}{\omega^2} \\ Q_{39} = a_{39} - \dfrac{c_{39}}{\omega^2} \\ Q_{93} = a_{93} - \dfrac{c_{93}}{\omega^2} \\ Q_{99} = m_{99} + a_{99} - \dfrac{c_{99}}{\omega^2}, \end{cases} \tag{17}$$

where m_{33} and m_{99} are the mass of the bodies, a_{33}, a_{39}, a_{93}, a_{99} are the added mass; b_{33}, b_{39}, b_{93}, b_{99} are the damping coefficients; B_{33} and B_{99} are the additional damping coefficients for the heave motions of the structure and the piston; c_{33}, c_{39}, c_{93}, c_{99} are the restoring force coefficients; f_3, f_9 are the complex excitations of the heave motions of two bodies; v_3, v_9 are the complex heave motion velocity amplitudes of the two bodies; A_0 is the sectional area of the water column; and p is the complex amplitude of the chamber pressure.

For the two-body system, the flowrate driven by the IWS can be expressed as

$$q_w = A_0(v_9 - v_3), \tag{18}$$

which means the positive velocity of the piston heave motion will create a positive flowrate, but the positive velocity of the heave motion of the device is a negative flowrate driven by the IWS. This is in line with a positive flowrate through the PTO when the air is discharging.

Combining (12) and (18) yields a chamber pressure as

$$p = k_1 A_0 (v_9 - v_3)\left(1 - i\omega k_1 \frac{V_0}{\gamma p_0}\right) \Big/ C_1. \tag{19}$$

Applying the linear relation (10), we have

$$q_{pto} = A_0 (v_9 - v_3)\left(1 - i\omega k_1 \frac{V_0}{\gamma p_0}\right) \Big/ C_1. \tag{20}$$

Substituting (19) into (16) yields

$$\begin{cases} [i\omega Q_{33} + b_{33} + B_{33}]v_3 + [i\omega Q_{39} + b_{39}]v_9 = f_3 + k_1 A_0^2 (v_9 - v_3)\left(1 - i\omega k_1 \dfrac{V_0}{\gamma p_0}\right) \Big/ C_1 \\ [i\omega Q_{93} + b_{93}]v_3 + [i\omega Q_{99} + b_{99} + B_{99}]v = f_9 - k_1 A_0^2 (v_9 - v_3)\left(1 - i\omega k_1 \dfrac{V_0}{\gamma p_0}\right) \Big/ C_1. \end{cases} \tag{21}$$

Rewriting the above equation yields

$$\begin{cases} [i\omega(Q_{33} - k_1^2 C_0/C_1) + (b_{33} + B_{33} + k_1 A_0^2/C_1)]v_3 + [i\omega(Q_{39} + k_1^2 C_0/C_1) + (b_{39} - k_1 A_0^2/C_1)]v_9 = f_3 \\ [i\omega(Q_{93} + k_1^2 C_0/C_1) + (b_{93} - k_1 A_0^2/C_1)]v_3 + [i\omega(Q_{99} - k_1^2 C_0/C_1) + (b_{99} + B_{99} + k_1 A_0^2/C_1)]v_9 = f_9, \end{cases} \tag{22}$$

where

$$C_0 = A_0^2 \frac{V_0}{\gamma p_0}. \tag{23}$$

It clearly shows that in the case of a constant PTO damping coefficient k_1 (see Eq. (10)), the equivalent damping coefficient is given by k_1/C_1 due to air compressibility, which is a reduced damping coefficient for PTO power conversion (but not necessarily for reducing power conversion!). Another significant effect of air compressibility is the increase in the spring coefficient (note: adding the negative values to Q_{33} and Q_{99} means the increases in the corresponding spring coefficients, and adding the positive values to Q_{39} and Q_{93} means the decreases in the coupled spring coefficients). It will be seen later in the examples below that air compressibility may indeed induce very complicated phenomena in the dynamic system.

The solution of Equation (22) can be given as

$$v_9 - v_3 = \frac{Z_1 + iZ_2}{\left(X_1 + X_2 k_1 A_0^2/C_1 + \omega^2 Y_2 k_1^2 C_0/C_1\right) + i\omega\left(Y_1 + Y_2 k_1 A_0^2/C_1 - X_2 k_1^2 C_0/C_1\right)} \tag{24}$$

and the IWS motion is given by

$$X_9 - X_3 = \frac{v_9 - v_3}{i\omega}, \tag{25}$$

with

$$\begin{cases} Z_1 = f_{9R}(b_{33} + B_{33} + b_{39}) - f_{3R}(b_{99} + B_{99} + b_{93}) - \omega f_{9I}(Q_{33} + Q_{39}) + \omega f_{3I}(Q_{99} + Q_{93}) \\ Z_2 = \omega f_{9R}(Q_{33} + Q_{39}) + f_{9I}(b_{39} + b_{33} + B_{33}) - \omega f_{3R}(Q_{99} + Q_{93}) - f_{3I}(b_{99} + B_{99} + b_{93}) \\ X_1 = (b_{33} + B_{33})(b_{99} + B_{99}) - b_{93}b_{39} - \omega^2(Q_{33}Q_{99} - Q_{93}Q_{39}) \\ X_2 = b_{33} + b_{99} + b_{39} + b_{93} + B_{33} + B_{99} \\ Y_1 = (b_{33} + B_{33})Q_{99} + (b_{99} + B_{99})Q_{33} - b_{93}Q_{39} - b_{39}Q_{93} \\ Y_2 = Q_{33} + Q_{99} + Q_{39} + Q_{93}, \end{cases} \tag{26}$$

where f_{3R} and f_{9R} are the real parts of the excitations f_3 and f_9, and f_{3I} and f_{9I} are the imaginary parts of the excitations f_3 and f_9.

The average power can be given by

$$\bar{P} = \frac{1}{2}\mathrm{Re}\left(p \times q_{pto}^*\right) = \frac{1}{2}k_1 A_0^2 (v_9 - v_3)(v_9 - v_3)^*/C_1 \tag{27}$$

or

$$\bar{P} = \frac{1}{2}k_1 A_0^2 \frac{\left(Z_1^2 + Z_2^2\right)/C_1}{\left(X_1 + X_2 k_1 A_0^2/C_1 + \omega^2 Y_2 k_1^2 C_0/C_1\right)^2 + \omega^2\left(Y_1 + Y_2 k_1 A_0^2/C_1 - X_2 k_1^2 C_0/C_1\right)^2}. \tag{28}$$

D. Floating OWC devices without air compressibility

Now a simplified case is studied below where the air compressibility is ignored. As such, the flowrate through the PTO can be simply calculated as

$$q_{pto} = A_0(v_9 - v_3). \tag{29}$$

For a linear PTO, the chamber pressure is expressed as

$$p = k_1 A_0 (v_9 - v_3). \tag{30}$$

The frequency domain dynamic equation can be given as

$$\begin{cases} [i\omega Q_{33} + (b_{33} + k_1 A_0^2)]v_3 + [i\omega Q_{39} + (b_{39} - k_1 A_0^2)]v_9 = f_3 \\ [i\omega Q_{93} + (b_{93} - k_1 A_0^2)]v_3 + [i\omega Q_{99} + (b_{99} + k_1 A_0^2)]v_9 = f_9, \end{cases} \tag{31}$$

and the average power is calculated as

$$\bar{P} = \frac{1}{2} k_1 A_0^2 \frac{Z_1^2 + Z_2^2}{\left(X_1 + X_2 k_1 A_0^2\right)^2 + \omega^2 \left(Y_1 + Y_2 k_1 A_0^2\right)^2}, \tag{32}$$

with the variables being defined in Eq. (26).

To optimise the PTO, we set

$$\frac{\partial \bar{P}}{\partial k_1} = 0, \tag{33}$$

which leads to the optimised linear PTO damping coefficient, as

$$k_1 = \frac{1}{A_0^2} \sqrt{\frac{X_1^2 + \omega^2 Y_1^2}{X_2^2 + \omega^2 Y_2^2}}. \tag{34}$$

So the capture power under the optimised PTO damping coefficient has a formula as

$$\bar{P}_{\max} = \frac{1}{4} \frac{Z_1^2 + Z_2^2}{X_1 X_2 + \omega^2 Y_1 Y_2 + \sqrt{\left(X_1^2 + \omega^2 Y_1^2\right)\left(X_2^2 + \omega^2 Y_2^2\right)}}. \tag{35}$$

This is the same formula as given by Sheng and Lewis,[34] which will be used for studying the optimisation of the PTO and the device in the floating OWC converter.

E. Fixed OWC devices with air compressibility

In this section, a case of a fixed OWC is considered. Similar to the convention used above, the internal water surface motion for power conversion in the fixed OWC can be considered as the result of the heave motion of the "imaginary piston," i.e., the heave motion of the water body. Hence, the dynamic equation can be expressed as

$$[i\omega Q_{99} + b_{99} + B_{99}]v_9 = f_9 - A_0 p. \tag{36}$$

For the fixed OWC, the flowrate driven by the IWS can be expressed as

$$q_w = A_0 v_9, \tag{37}$$

which means the positive velocity of the piston heave motion will create a positive flowrate driven by the IWS.

Combining (12) and (37) yields a chamber pressure as

$$p = k_1 A_0 v_9 \left(1 - i\omega k_1 \frac{V_0}{\gamma p_0}\right) \Big/ C_1. \tag{38}$$

Applying the linear relation (10), we have

$$q_{pto} = A_0 v_9 \left(1 - i\omega k_1 \frac{V_0}{\gamma p_0}\right) \Big/ C_1. \tag{39}$$

Substituting (38) into (36) yields

$$[i\omega(Q_{99} - k_1^2 C_0/C_1) + (b_{99} + B_{99} + k_1 A_0^2/C_1)]v_9 = f_9. \tag{40}$$

Again, it can be seen that in the case of a constant PTO damping coefficient k_1 (see Eq. (10)), the equivalent damping coefficient is given by k_1/C_1, and the effect of air compressibility increases the spring coefficient.

The solution of Equation (40) can be given as

$$v_9 = \frac{f_9}{i\omega\left(Q_{99} - k_1^2 C_0/C_1\right) + \left(b_{99} + B_{99} + k_1 A_0^2/C_1\right)}. \tag{41}$$

The average power can be given from Eqs. (38) and (39) as

$$\bar{P} = \frac{1}{2}\mathrm{Re}\left(p \times q_{pto}^*\right) = \frac{1}{2} k_1 A_0^2 v_9 v_9{}^* / C_1 \tag{42}$$

or

$$\bar{P} = \frac{1}{2} k_1 A_0^2 \frac{|f_9|^2/C_1}{\omega^2\left(Q_{99} - k_1^2 C_0/C_1\right)^2 + \left(b_{99} + B_{99} + k_1 A_0^2/C_1\right)^2}. \tag{43}$$

If air compressibility is not included, the flowrate through the PTO can be simply calculated as

$$q_{pto} = A_0 v_9. \tag{44}$$

So the chamber pressure is

$$p = k_1 A_0 v_9. \tag{45}$$

The dynamic equation for the OWC wave energy converter is

$$[i\omega Q_{99} + (b_{99} + B_{99} + k_1 A_0^2)]v_9 = f_9. \tag{46}$$

The solution of Equation (46) can be given as

$$v_9 = \frac{f_9}{i\omega Q_{99} + \left(b_{99} + B_{99} + k_1 A_0^2\right)}. \tag{47}$$

The average power is given as

$$\bar{P} = \frac{1}{2} k_1 A_0^2 \frac{|f_9|^2}{\omega^2 Q_{99}^2 + \left(b_{99} + B_{99} + k_1 A_0^2\right)^2}. \tag{48}$$

To optimise the PTO, we set

$$\frac{\partial \bar{P}}{\partial k_1} = 0, \tag{49}$$

which leads to the optimised linear PTO damping coefficient, as

$$k_1 = \frac{1}{A_0^2}\sqrt{\omega^2 Q_{99}^2 + (b_{99} + B_{99})^2}. \tag{50}$$

So the capture power under the optimised PTO damping coefficient has a formula as

$$\bar{P}_{\max} = \frac{1}{4}\frac{|f_9|^2}{b_{99} + B_{99} + \sqrt{\omega^2 Q_{99}^2 + (b_{99} + B_{99})^2}}. \tag{51}$$

This is the same formula as given by Sheng and Lewis[34] for a fixed point absorber.

III. TIME DOMAIN ANALYSIS

A. Time domain dynamic equation

As it has been shown in Section II, the frequency domain analysis can be only conducted if the PTO is linear, and this can only be done when a simplification (9) has been used. Recently, a more comprehensive and realisable process of air compressibility in the air chamber has been proposed by Sheng *et al.*[27] in which the hydrodynamics and the thermodynamics are coupled by employing the air turbine PTOs (linear and nonlinear) in time domain. This approach applies the conventional "hybrid-frequency/time-domain method,"[35] but couples the hydrodynamics and thermodynamics. Below are the coupled time domain equations for a floating OWC device (only both heave motions of the device itself and the water body are used for power conversion),

$$\begin{cases} [m_{33} + a_{33}(\infty)]\ddot{X}_3(t) + \int_0^t K_{33}(t-\tau)\dot{X}_3(\tau)d\tau + B_{33}\dot{X}_3(t) + C_{33}X_3(t) + a_{39}(\infty)\ddot{X}_9(t) \\ \quad + \int_0^t K_{39}(t-\tau)\dot{X}_9(\tau)d\tau + C_{39}X_9(t) = F_3(t) + A_0 p(t) \\ a_{93}(\infty)\ddot{X}_3(t) + \int_0^t K_{93}(t-\tau)\dot{X}_3(\tau)d\tau + C_{93}X_3(t) + [m_{99} + a_{99}(\infty)]\ddot{X}_9(t) \\ \quad + \int_0^t K_{99}(t-\tau)\dot{X}_9(\tau)d\tau + B_{99}\dot{X}_9(t) + C_{99}X_9(t) = F_9(t) - A_0 p(t), \end{cases} \tag{52}$$

where $a_{33}(\infty)$, $a_{39}(\infty)$, $a_{93}(\infty)$, and $a_{99}(\infty)$ are the added masses for the heave motions for the first and second bodies and their coupling terms at the infinite frequency; K_{33}, K_{99} and K_{93}, K_{39} are the impulse functions for heave motions and their coupling terms; C_{33}, C_{99} and C_{93}, C_{39} are the restoring force coefficients and their coupling terms; F_3 and F_9: the excitations for the first and second bodies, X_3 and X_9: the heave motions for the first and second bodies; and $p(t)$: the instantaneous gauge pressure in the air chamber.

The flowrate driven by the IWS is calculated as

$$q_w(t) = A_0(\dot{X}_9 - \dot{X}_3), \tag{53}$$

and once the pressure is resolved from the time-domain equation, the flowrate through the PTO can be calculated either using (8) or (9).

B. Calculation of the memory effects

The memory effects in (52) can be calculated using the modified Prony's method developed by Sheng *et al.*,[36] in which a recursive calculation replaces the convolution calculation. For a completeness, the method is given here.

First, the impulse response function can be approximated using an exponential fitting using the Prony's function as

$$K(t) \approx \sum_{k=1}^{N} \alpha_k e^{\beta_k t}, \tag{54}$$

where N is the order of the exponential function or the order of Prony function, and α_k and β_k are the complex coefficients which can be obtained from the Prony method (the details of the method can be found in Ref. 37).

The memory effect can then be expressed as

$$I(t) = \int_0^t K(t-\tau)\dot{X}(\tau)d\tau = \sum_{k=1}^{N} \alpha_k e^{\beta_k t} \int_0^t e^{-\beta_k \tau}\dot{X}(\tau)d\tau. \tag{55}$$

The memory effect is calculated from the starting time ($\tau = 0$) to the present time ($\tau = t$).

Let

$$I(t) = \sum_{k=1}^{N} I_k(t) \tag{56}$$

with

$$I_k(t) = \alpha_k e^{\beta_k t} \int_0^t e^{-\beta_k \tau}\dot{X}(\tau)d\tau. \tag{57}$$

For the sampled system, a recursive formula is given as

$$I_k(n+1) = I_k(n)e^{\beta_k \Delta t} + \dot{X}(n)\Delta t \alpha_k e^{\beta_k \Delta t/2}. \tag{58}$$

C. Linear power take-off (k_1)

For a linear PTO governed by Eq. (8), the thermodynamics equation is given by

$$\dot{p} + (\gamma p_0 + p)\frac{\dot{V}}{V} + \frac{\gamma p_0}{V}\frac{p}{k_1} = 0. \tag{59}$$

This is the dynamic equation for the air chamber volume and the chamber pressure forming a closed dynamic system because of the application of the PTO. If the chamber volume is known (for example, the internal water surface motion is known), then the chamber pressure can be resolved for the given PTO, and vice versa.

The air chamber volume is calculated as

$$V = V_0 - A_0(X_9 - X_3). \tag{60}$$

This equation is the link between the hydrodynamics and thermodynamics of the OWC device.

D. Nonlinear power take-off (k_2)

For an orifice PTO, the general relation of the chamber pressure and the mass flowrate through the PTO is a parabolic relation, and the mathematical expressions are as follows:

$$p = \pm k_2 q_{pto}^2, \tag{61}$$

where k_2 is the mass flowrate damping coefficient and $\pm$ means exhalation and inhalation, respectively.

Similarly, the combination of the PTO equation and (8) can lead to the thermodynamic equations as follows:
for exhalation

$$\dot{p} + (\gamma p_0 + p)\frac{\dot{V}}{V} + \frac{\gamma p_0}{V}\sqrt{\frac{p}{k_2}} = 0, \tag{62}$$

for inhalation

$$\dot{p} + (\gamma p_0 + p)\frac{\dot{V}}{V} - \frac{\gamma p_0}{V}\sqrt{\frac{-p}{k_2}} = 0. \tag{63}$$

E. Capture power

Once the time domain equations are solved, then the capture power from waves to pneumatic power is given by

$$P(t) = p(t) \times q_{pto}(t), \tag{64}$$

and the average power output is calculated as

$$\bar{P} = \frac{1}{T}\int_0^T P(t)dt, \tag{65}$$

where T is the time interval for calculating the average power.

IV. CAPTURE POWER IN IRREGULAR WAVES

Real ocean waves are significantly different from those regular waves of unique wave height and period. When the real ocean waves are referred, they are normally characterised by the significant wave height (H_s), a characteristic period (T_c), and the corresponding spectrum shape. The significant wave height is well defined either in frequency domain as

$$H_s = 4\sqrt{m_0}, \tag{66}$$

with m_0 being the zero-order of the spectral moment, given with $n = 0$ from the nth-order spectral moment

$$m_n = \int_0^\infty S_w(\omega)\omega^n d\omega, \tag{67}$$

where $S_w(\omega)$ is the wave spectrum.

In time-domain analysis, $H_{1/3}$, calculated as the averaged value of the one-third highest wave heights, is frequently referred as the significant wave height, though these two definitions may give slightly different results in practical cases.

Relatively, the characteristic period can be one of many definitions, including energy period (T_e), peak spectral period (T_p), spectral mean period (T_{01}), and zero up-crossing period (T_z), and the choice of a characteristic period to represent the sea state may be subject to the situation. For example, if the wave energy is the topic, the energy period may be very useful,

while to define the wave spectrum, the peak period, T_p, or the spectrum mean period, T_{01}, is frequently used. The above periods may be the most used characteristic periods, and for the Bretschneider or JONSWAP spectrum, these characteristic periods have the following fixed relations regardless of the wave height and period:

$$\begin{cases} T_e = 0.857T_p \\ T_{01} = 0.772T_p \\ T_z = 0.710T_p, \end{cases} \tag{68}$$

where the Bretschneider spectrum is defined as

$$S_w(\omega) = \frac{5}{16}\frac{\omega_p^4}{\omega^5}H_s^2 \exp\left(-\frac{5}{4}\frac{\omega_p^4}{\omega^4}\right), \tag{69}$$

where $\omega_p = \frac{2\pi}{T_p}$.

The characteristic periods are given as

$$T_e = 2\pi\frac{m_{-1}}{m_0}, \quad T_{01} = 2\pi\frac{m_0}{m_1}, \quad T_z = 2\pi\sqrt{\frac{m_0}{m_2}}. \tag{70}$$

Once the power curve is obtained, then the capture power in irregular waves for a constant optimised PTO damping coefficient can be calculated (see Sheng and Lewis[38]) as

$$P_{irr} = 2\int_0^\infty \bar{P}S_w(\omega)d\omega, \tag{71}$$

where $\bar{P}$ is given by Eq. (28) for the case with air compressibility or by Eq. (32) for the case without air compressibility.

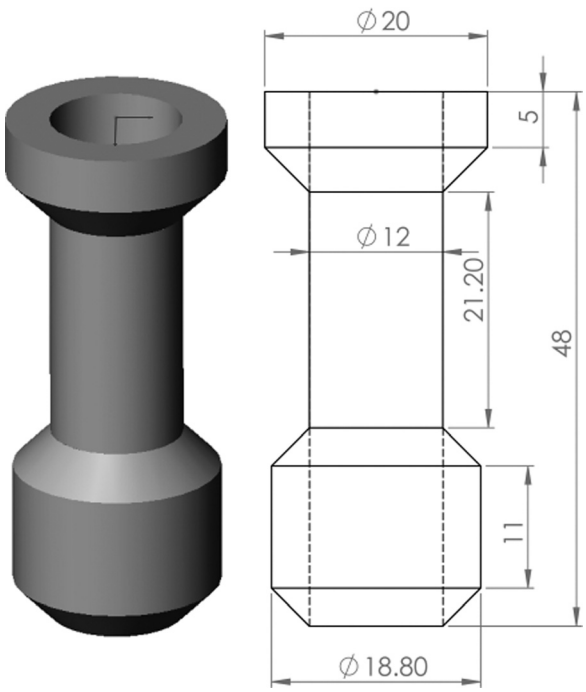

FIG. 1. A cylindrical OWC wave energy converter (submerged part).

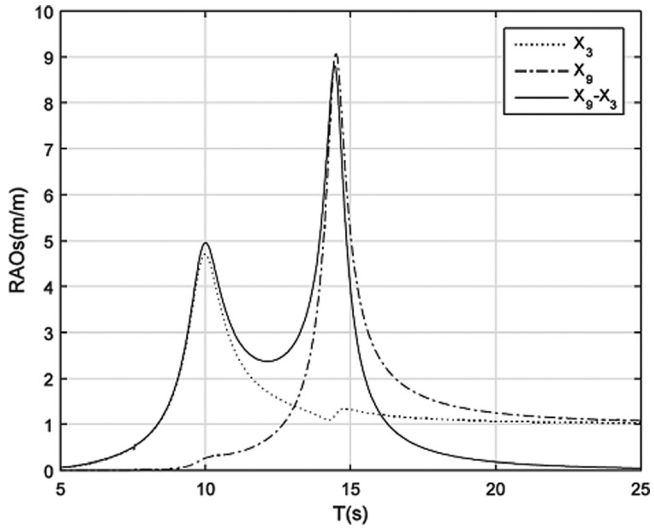

FIG. 2. Heave RAOs of the structure (X_3) and the water body (X_9) and their relative motion RAO (X_9-X_3), with additional damping coefficients: $B_{33} = 200$ kN s/m and $B_{99} = 100$ kN s/m.

V. EXAMPLES AND ANALYSIS

The studied OWC can be seen in Figure 1, which is a similar OWC studied by Gomes *et al.*,[39] and further studied by Sheng and Lewis.[40] The floating OWC device has a displacement of 3609 m^3 with the resonance periods of the heave motions of the structure and the water body in the water column being 9.94 s and 14.35 s, respectively (Figure 2), in which the relative response (X_9–X_3) is also given. In the study, the heave motions/responses of both the structure and the "imaginary piston" have been damped using the additional damping coefficients for the heave motions ($B_{33} = 2 \times 10^5$ N s/m and $B_{99} = 10^5$ N s/m) so that both heave responses have reasonable amplitudes. From the figure, it can be seen that the floating OWC may convert the energy from waves of periods of 10–14.5 s efficiently.

In the OWC device, the air chamber is assumed to have a height of 10 m, which corresponds to the volumetric ratio Vr = 1.0. In this study, varying Vr means a change in the air chamber height (e.g., Vr = 0.5 for 5 m, Vr = 1.5 for 15 m, etc.).

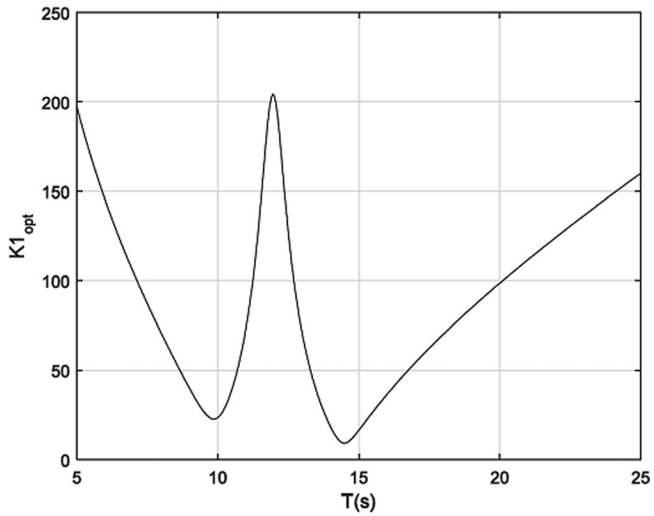

FIG. 3. Optimised damping coefficients for the linear PTO (K_1) for the floating OWC.

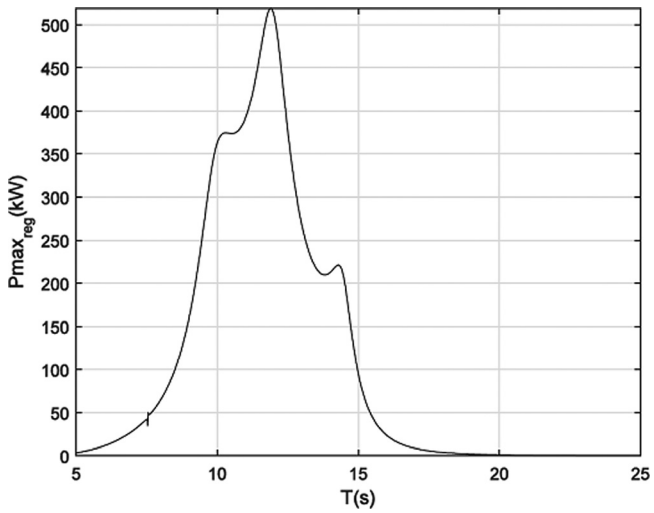

FIG. 4. Maximal power conversion for the floating OWC for different wave periods.

A. PTO damping optimisations (without air compressibility)

Based on the formula (34), the optimised PTO damping coefficient for the floating OWCs is given in Figure 3. It can be seen that the overall trends in the optimised damping coefficients are very similar to those floating absorbers. Generally, for the floating OWC, the optimised damping coefficient has two local minimums which correspond to the two resonances of the structure and the IWS, respectively. From Figure 4, it can be seen that the power conversion has a wide bandwidth and the global maximum of the average power is more than 500 kW.

B. Responses with and without PTO

By applying a constant PTO coefficient to the floating OWC, the heave motions of the structure (X_3) and of the piston (X_9) and their relative motion, i.e., the IWS motion (X_9-X_3), have all been changed. From Figure 5(a), it can be seen that the heave response of the structure is reduced when the wave period is smaller than 12 s, and the largest reduction of the heave response happens around 10 s where the structure resonance is. When the wave period is larger than 12 s, the heave motion is increased due to the fact of the interaction of the structure and piston. For the piston motion, when the wave period is larger than 13 s, the motion response is reduced, especially a large response reduction happening at 14.35 s where the piston has a resonance in Figure 5(b). When the wave period is smaller than 13 s, the piston response is increased due to the PTO, and also the interaction between the structure and the piston. If the

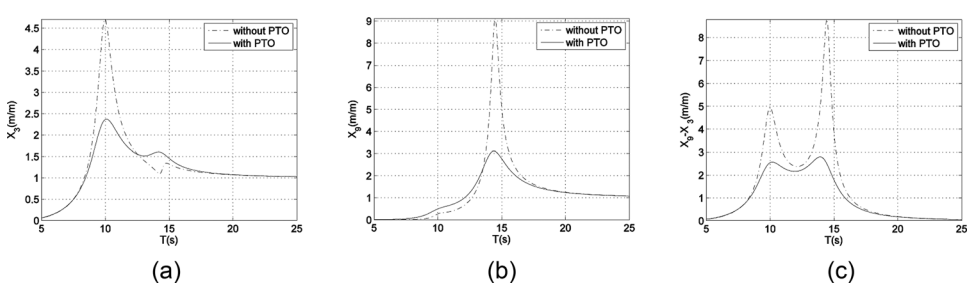

FIG. 5. Motion responses with and without PTO ($K_1 = 23.35\,N\,s/m^5$). (a) Heave motion responses of the structure; (b) Heave motion responses of the piston; and (c) IWS motion responses.

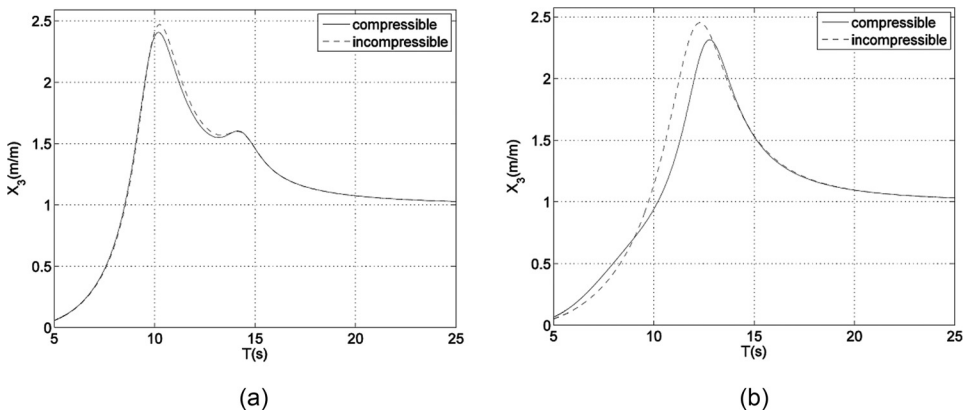

FIG. 6. Response comparison of the structure motions (with and without air compressibility) (a) $K_1 = 23.35\,N\,s/m^5$ (b) $K_1 = 101.15\,N\,s/m^5$.

relative motion is examined, it can be seen that the IWS motion is reduced for all the wave periods in Figure 5(c).

C. Dynamic responses and air compressibility

Now, we will examine the effect of the PTO damping coefficients on air compressibility. As shown in (22), the significant effects of air compressibility maybe the subtractions or additions in the mass terms in the dynamic equations. From the dynamic equation, it can be seen that the mass subtractions/additions are generally proportional to the volume of the air chamber, to the squares of the sectional area of the water column and of the PTO damping coefficient. For a wave condition of $H_s = 2\,m$ and $T_p = 10\,s$, the optimised damping coefficients can be calculated for the corresponding characteristic periods T_p, T_e, T_{01}, and T_z which are actually for the same sea state in different forms. Based on these periods, the supposed optimised PTO damping coefficients are $23.35\,N\,s/m^5$, $52.48\,N\,s/m^5$, $79.65\,N\,s/m^5$, and $101.15\,N\,s/m^5$, respectively, and these "optimised PTO damping coefficients" will be used for further analysis.

To show air compressibility, the smallest and largest damping coefficients are chosen regardless of whether they correspond to the maximum of capture power. It can be seen from Figures 6(a), 7(a), and 8(a), for the smallest PTO damping coefficient ($K_1 = 23.35\,N\,s/m^5$), the responses of the structure (X_3) and the piston (X_9) and the IWS (X_9-X_3) are all very similar for the cases with and without air compressibility, only very small differences can be discerned. For the case of the largest PTO damping coefficient ($K_1 = 101.15\,N\,s/m^5$), the structure (X_3) has normally smaller responses in the compressible case for most wave periods, unless the wave periods are

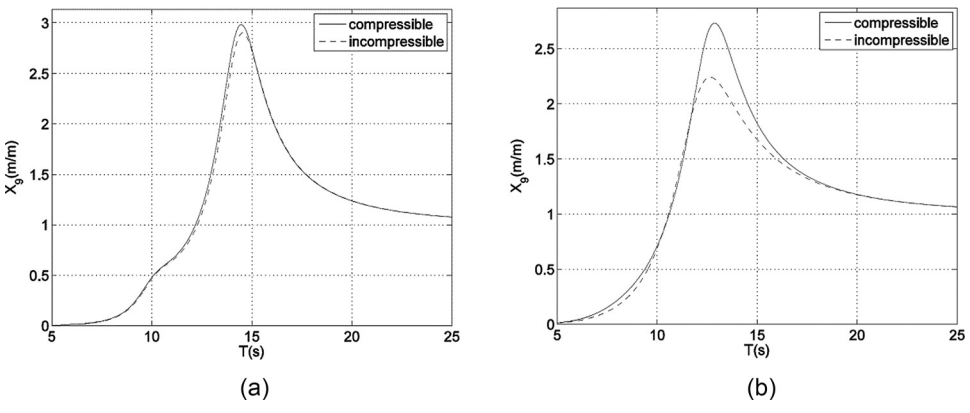

FIG. 7. Response comparison of the water body motions (with and without air compressibility) (a) $K_1 = 23.35\,N\,s/m^5$ (b) $K_1 = 101.15\,N\,s/m^5$.

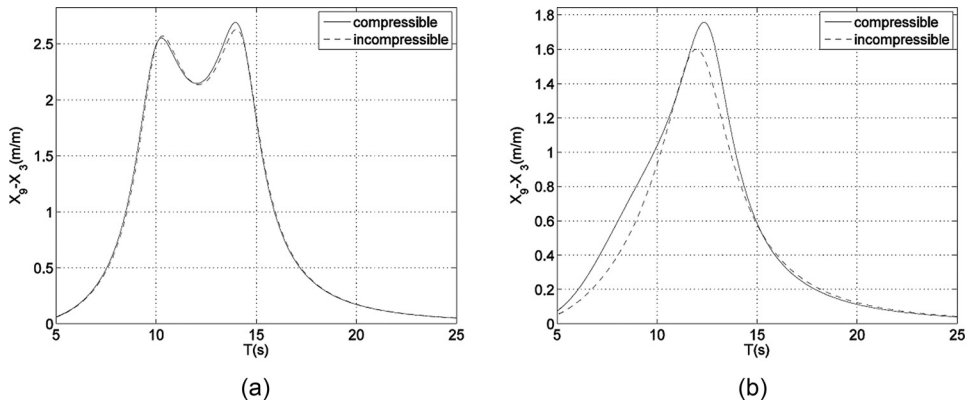

FIG. 8. Response comparison of the internal water surface motions (with and without air compressibility) (a) $K_1 = 23.35\,N\,s/m^5$ (b) $K_1 = 101.15\,N\,s/m^5$.

quite small (less than about 9 s, see Figure 6(b)). It is also noted that the heave response has a larger resonance period. For the "piston," it has larger responses in the compressible case for all wave periods, see Figure 7(b), and again the resonance period is slightly larger than that in the incompressible case. As the relative motion of the above heave motions, the IWS response is generally larger in the compressible than that in the incompressible case, see Figure 8(b).

A further comment is made to the increased resonance periods for both the structure and the piston. It must be noted that these two motion modes are interacted with each other, especially when the PTO is applied. Hence, the subtraction of the added mass in the self-mass term and the addition of the added mass in the cross-mass term due to air compressibility must be considered together and the analysis is not so straightforward as that of a single motion mode in the fixed OWC where the air compressibility simply reduces the overall mass in the dynamic system. In addition, due to air compressibility, the actual PTO damping coefficient is reduced (see Eq. (22)). Hence, the interaction between the two bodies can be more complicated in this regard.

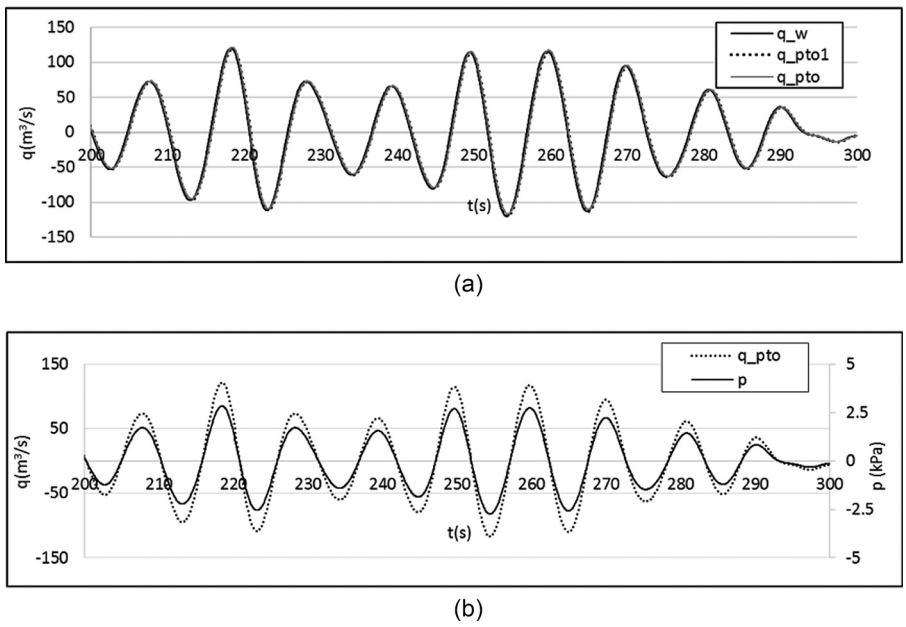

FIG. 9. A comparison of the flowrates through the PTO ("q_pto" by Eq. (8) and "q_pto1" by Eq. (9)) and the flowrate driven by the IWS (Eq. (7)). Vr = 1.0, Hs = 2.0 m and $T_p = 10$ s, $K_1 = 23.35\,N\,s/m^5$, P_av = 67.79 kW (floating). (a) Comparison of flowrates and (b) flowrate and chamber pressure.

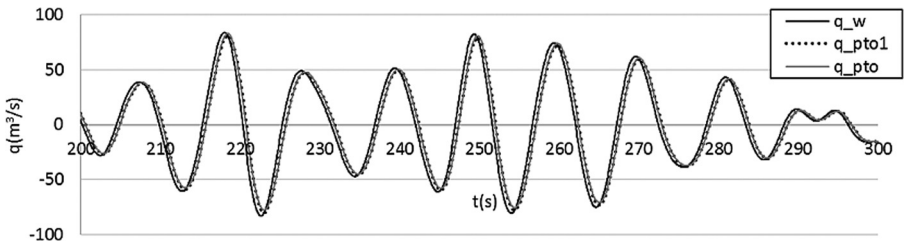

FIG. 10. A comparison of the flowrates through the PTO ("q_pto" by Eq. (8) and "q_pto1" by Eq. (9)) and the flowrate driven by the IWS (Eq. (7)). Vr = 1.0, Hs = 2.0 m, and T_p = 10 s, K_1 = 52.48 N s/m^5, P_av = 80.27 kW (floating).

D. Air flow with air compressibility

In the case of a small PTO damping coefficient, $K_1 = 23.35$ N s/m^5, the flowrate driven by the IWS and the flowrate through the PTO are very close in Figure 9(a). For a comparison, the flowrates calculated by Eq. (8), "q_pto," and the simplified formula (9), "q_pto1," are both plotted. For a comparison, the flowrate driven by the IWS is also given as "q_w." The closeness of all three flowrates means a very small air compressibility and a good approximation of the formula (9). In Figure 9(b), the chamber pressure and the flowrate through the PTO are plotted together to show a perfect agreement in phase between the chamber pressure and the flowrate through PTO.

With an increased PTO damping coefficient (K_1 from 23.35 to 52.48 N s/m^5), the power conversion reaches a maximum. Due to the increased K_1, the flowrates reduce when compared to the case of a small damping coefficient (Figure 10). However, it can be seen that there is a small phase difference between the flowrate driven by the IWS and the flowrate through the PTO, which is an indicator of a weak air compressibility, performing like a "spring effect." Though Eq. (9) is a simplified form for the air compressibility, its flowrate is very close to that from Eq. (8).

To examine more air compressibility, we further increase the air chamber volume by 5 times (i.e., Vr = 5), as such the air compressibility can be significant (Figure 11(a)) in which we can see that the flowrate driven by the IWS is very different from those through the PTO

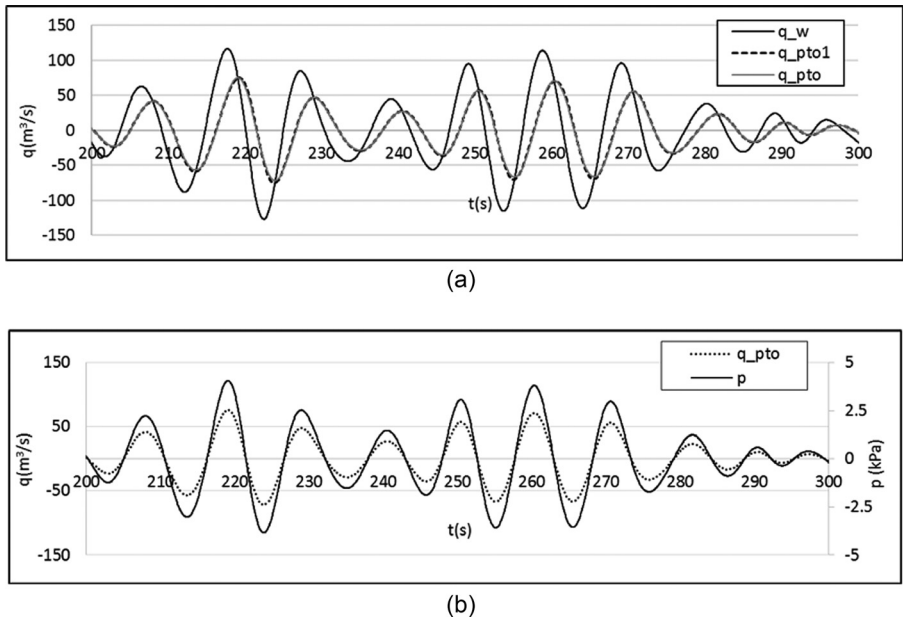

FIG. 11. A comparison of the flowrates through the PTO ("q_pto" by Eq. (8) and "q_pto1" by Eq. (9)) and the flowrate driven by the IWS (Eq. (7)). Vr = 5.0, Hs = 2.0 m, and T_p = 10 s, K_1 = 52.48 N s/m^5, P_av = 65.25 kW (floating). (a) Comparison of flowrates and (b) flowrate and chamber pressure.

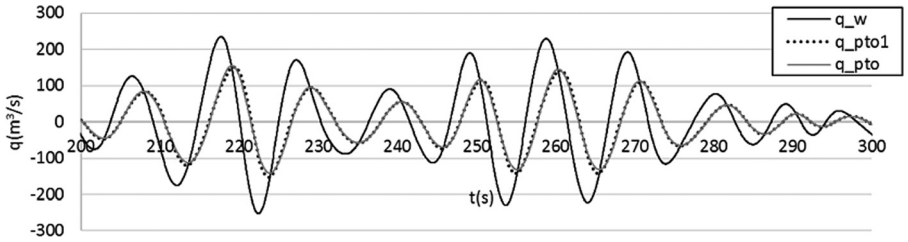

FIG. 12. A comparison of the flowrates through the PTO ("q_pto" by Eq. (8) and "q_pto1" by Eq. (9)) and the flowrate driven by the IWS (Eq. (7)). Vr = 5.0, Hs = 4.0 m and $T_p = 10$ s, $K_1 = 52.48$ N s/m^5, P_av = 261.26 kW (floating).

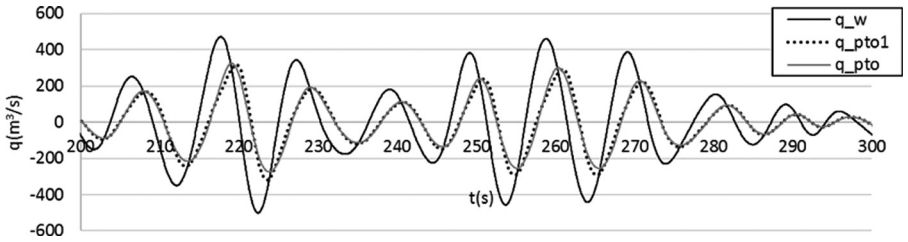

FIG. 13. A comparison of the flowrates through the PTO ("q_pto" by Eq. (8) and "q_pto1" by Eq. (9)) and the flowrate driven by the IWS (Eq. (7)). Vr = 5.0, Hs = 8.0 m, and $T_p = 10$ s, $K_1 = 52.48$ N s/m^5, P_av = 1049.1 kW (floating).

("q_pto" and "q_pto1") in both amplitude and phase. Due to air compressibility, the flowrate through the PTO is significantly reduced when compared to the flowrate driven by the IWS. Again, with evident air compressibility, the simplified flowrate formula (9) is still a very good approximation to the formula (8). In Figure 11(b), the flowrate "q_pto" and the chamber pressure show a perfect phase agreement.

Figures 12 and 13 show the flowrates for the cases of the increased wave heights ($H_s = 4$ m and $H_s = 8$ m, respectively, compared to $H_s = 2$ m in the previous example). In both cases, the air compressibility can obviously be seen. In the case of $H_s = 4$ m, the flowrates using Eqs. (8) and (9) are still very close, with small differences at the large peaks and troughs, even in the case of a very high sea state of $H_s = 8$ m. Hence, it can be generally concluded that the Sarmento's simplification[26] is a very good approximation and linearisation.

Another interesting result can be seen in Figure 14. When varying the wave height from $H_s = 2$ m to $H_s = 8$ m whilst keeping all other parameters unchanged, the flowrate through the PTO is very linear to the wave height: if the flowrate in $H_s = 2$ m times 4 (wave height increased 4 times), the flowrates in both cases are almost identical, with small differences discernible at the peaks and troughs.

E. Chamber pressure and air compressibility

In Figure 15, a comparison has been made for the flowrates for different PTO damping coefficients and air chamber volumes. For the case of normal air chamber where Vr = 1 (i.e.,

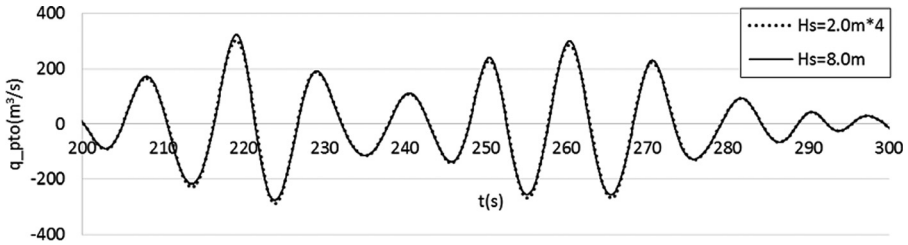

FIG. 14. PTO flowrate scaling-up ($T_p = 10$ s, $K_1 = 52.48$ N s/m^5).

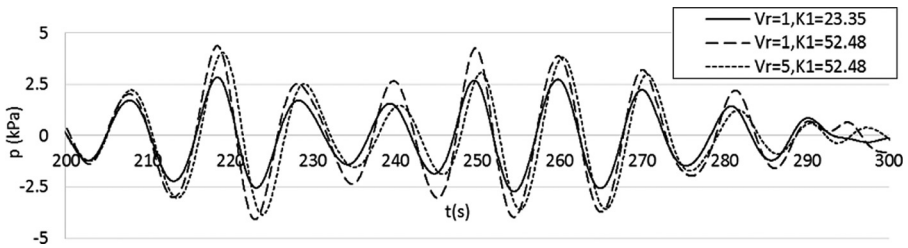

FIG. 15. Hs = 2.0 m, $T_p = 10$ s.

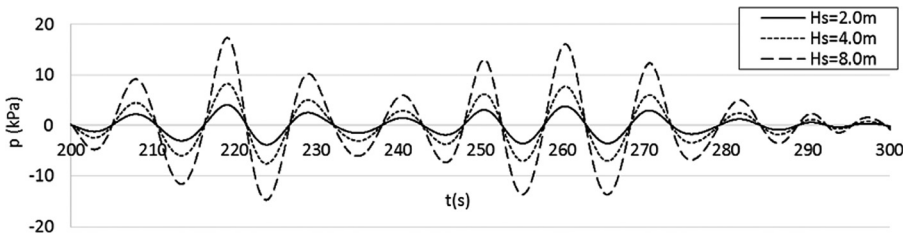

FIG. 16. $T_p = 10$s, Vr = 5.0, and K1 = 52.48 N s/m^5.

the air chamber height is 10 m), with different PTO damping coefficients ($K_1 = 23.35$ and 52.48 N s/m^5, respectively), the chamber pressures are generally in phase with each other ("black line" and "red line"), but have different amplitudes. It should be understandable that a large damping PTO coefficient means a large blockage of the air flow through the PTO, thus a higher chamber pressure is created. However, if the air chamber volume is increased from Vr = 1 to Vr = 5, then the chamber pressure ("green line") has a lag in the phase, and also the pressure amplitude is reduced due to a larger air compressibility.

Figure 16 shows a comparison of the chamber pressures for different wave heights. Generally, the chamber pressures are in a very good agreement in phase, but the amplitudes are increased with the increase of the wave heights. Figure 17 shows a comparison of the chamber pressure for the wave heights of $H_s = 2$ m and $H_s = 8$ m, but the pressure for $H_s = 2$ m is enlarged by 4. It can be seen that these two pressures are very close, and small differences can be seen only at the large peaks and troughs.

F. Air compressibility and power conversion

Table I shows the power conversions for the OWC with different air chambers and for different PTO damping coefficients. For a particular wave condition ($H_s = 2$ m and $T_p = 10$ s), the power conversions reach maximum for Vr = 1.5 for both PTO damping coefficients. Table II gives the optimised air turbine damping coefficient and the corresponding capture power for different air volumes. Again, for air volume ratio Vr = 1.5, maximal capture power is attained though it is only marginally larger than the case of Vr = 1.0.

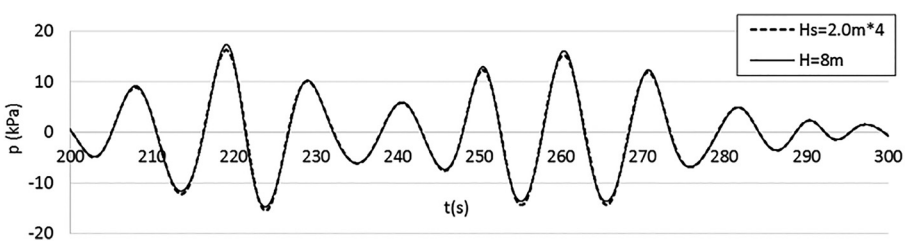

FIG. 17. Pressure scaling-up ($K_1 = 52.48$ N s/m^5).

TABLE I. Capture power (P_irr, kW) from irregular waves for the floating OWC (Hs = 2.0 m, Tp = 10 s).

	Vr = 0.5	Vr = 1.0	Vr = 1.5	Vr = 2.5	Vr = 5.0	Vr = 10.0
$K_1 = 23.35\ N\ s/m^5$	57	67.12	67.15	66.64	62.25	46.63
$K_1 = 52.47\ N\ s/m^5$	78.51	79.35	79.63	78.30	65.94	36.66

TABLE II. Optimised damping and capture powers for different air volumes (Hs = 2.0 m, Tp = 10 s).

	Vr = 0.5	Vr = 1.0	Vr = 1.5	Vr = 2.5	Vr = 5.0	Vr = 10.0
K_1 (N s/m^5)	57.60	62.15	62.28	62.15	40.07	22.53
P_irr (kW)	78.55	79.54	79.94	78.43	66.83	46.62

A further examination is made to the maximal power conversions for the OWC with different air chambers. From Figure 18, it can be seen that Vr = 1.5 gives best result, but it is very close to the capture powers for Vr less than 2.5. Further increasing the air chamber volume, the power conversion will be significantly reduced.

G. Nonlinear PTO and air compressibility

One interesting aspect may be the effects of the nonlinearities of the PTO to air compressibility and power conversion. In the first case, the normal air chamber (Vr = 1.0) and the waves of $H_s = 2.0$ m and $T_p = 10$ s are considered. In the comparison, the optimised damping coefficients ($K_1 = 52.48\ N\ s/m^5$) and ($K_2 = 1.16\ N\ s^2/m^8$) are both chosen such that the OWC can take the maximum mean power from waves: 80.19 kW and 80.13 kW, with the ratios of the maximum instantaneous power and the mean power are 13.23 and 13.98, respectively (linear PTO and nonlinear PTO). It can be seen that for the optimised damping coefficients, both linear and nonlinear PTOs provide almost the same power conversion, which is a conclusion made by Sheng and Lewis.[40]

In Figure 19, the flowrates driven by the IWS are compared for the linear and nonlinear PTOs. It can be seen that both flowrates driven by the IWS are very close. However, the flowrates passing through the PTOs can be different (see Figure 20). The flowrate through the linear PTO has larger maximal values in peaks and troughs, and small differences can be discerned near zero. Corresponding to the different flowrates through the PTOs, the chamber pressures are different for the linear and nonlinear PTOs (Figure 21). In addition to the larger pressure

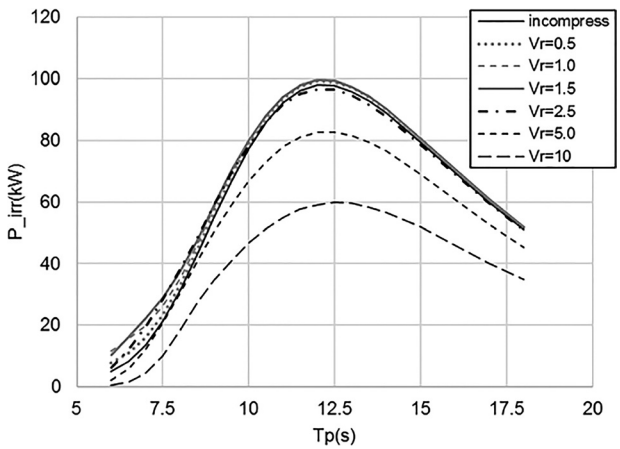

FIG. 18. Power conversions for different air chambers.

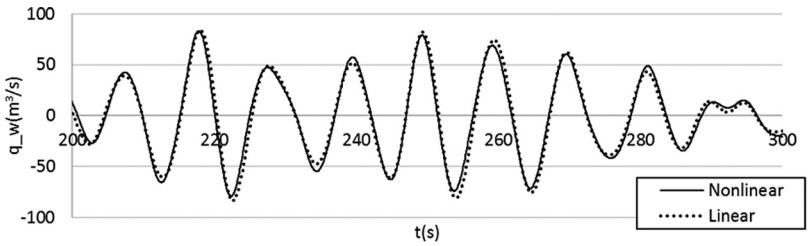

FIG. 19. Flowrates driven by the IWS for linear and nonlinear PTOs: Hs = 2 m and Tp = 10 s.

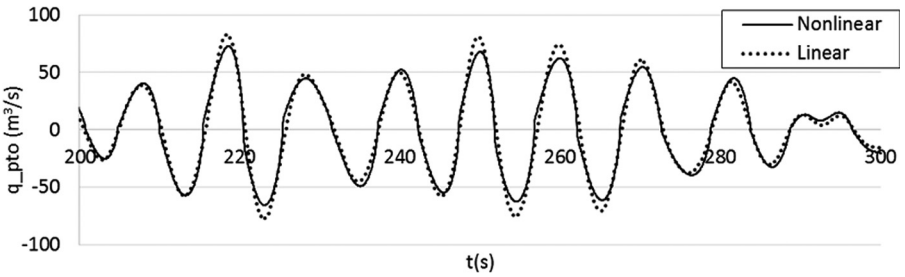

FIG. 20. Flowrates through PTOs for linear and nonlinear PTOs: Hs = 2 m and Tp = 10 s.

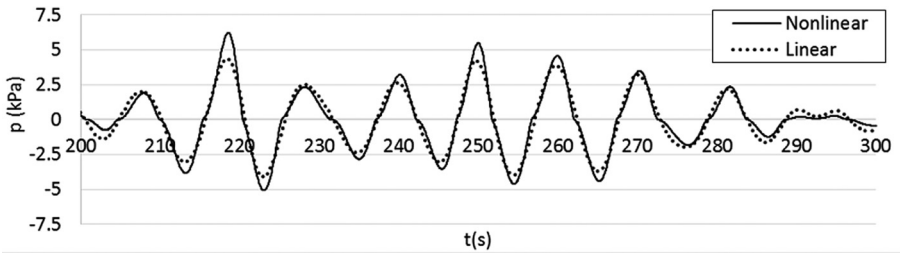

FIG. 21. Chamber pressures for linear and nonlinear PTOs: Hs = 2 m and Tp = 10 s (floating).

amplitudes for the nonlinear PTO, it also presents the nonlinear transitions around zeros. When it comes to the power conversion (Figure 22), the nonlinear PTO has a higher maximal capture power; hence, the ratios of the maximum power and the average power are slightly different (13.97 vs. 13.23).

When the air chamber volume is increased to 5 times larger (i.e., Vr = 5). The flowrates driven by the IWS are increased significantly (compare Figures 23 and 19), and again, the PTO type has a small influence on the flowrate driven by the IWS. However, the flowrates passing through the PTOs are reduced due to air compressibility, and in which the flowrate through the

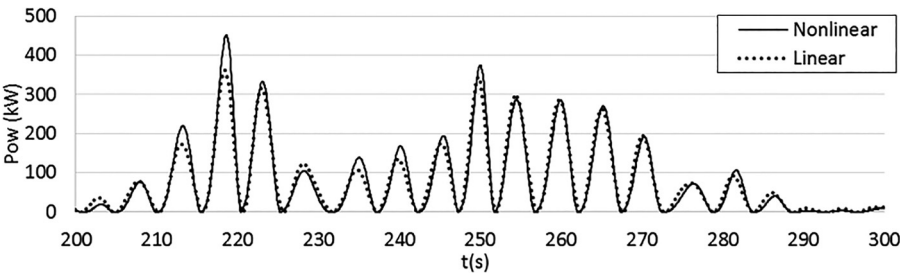

FIG. 22. Capture powers for linear and nonlinear PTOs: Hs = 2 m and Tp = 10 s (floating).

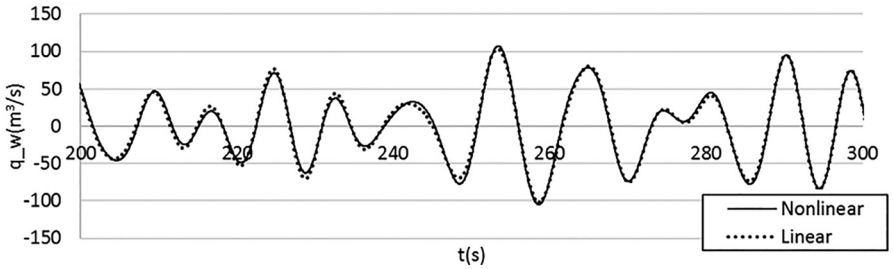

FIG. 23. Flowrates driven by internal water surfaces.

linear PTO has larger values when the flowrate is large, but smaller when the flowrate is small when compared to the nonlinear PTO (Figure 24). It is also noted that the flowrate passing through the nonlinear PTO is no longer linear even though the flowrate driven by the IWS remains linear.

Due to the air compressibility, the chamber pressures become smoother with the nonlinear PTO, and there is no significant transitions of the chamber pressure across zeros (it is very similar to the chamber pressure with a linear PTO, see Figure 25). Accordingly, the reduced chamber pressure and flowrates through the PTOs lead to reduced capture powers: 65.33 kW for linear PTO and 63.48 kW for nonlinear PTO (see Figure 26), with the power conversion ratios 11.46 and 10.42, respectively.

VI. AIR COMPRESSIBILITY IN A FIXED OWC

In the section, air compressibility problem will be studied for a fixed OWC device and as a comparison to the floating OWC. To make a valid comparison to the floating OWC, the draft of the fixed OWC is reduced to 20.50 m (Figure 27) so that the resonance period of the internal water surface is reduced to 10 s, similar to the lower resonance period of the IWS in the floating OWC. For studying the fixed OWC, the shortened device can simply be taken as a fixed structure. For power conversion, the passing wave excites the internal water surface (IWS) to move up and down which can be used to drive an air flow in the air chamber, and thus a chamber pressure at the presence of a PTO.

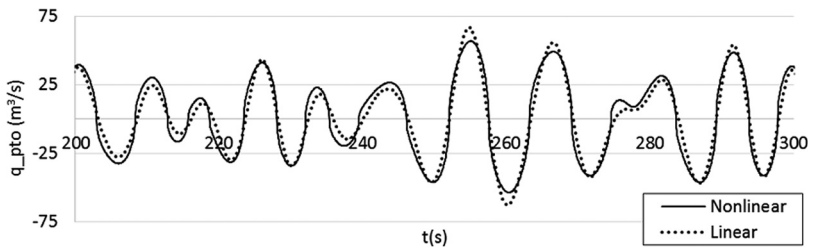

FIG. 24. Flowrates through the linear and nonlinear PTOs: Hs = 2 m and Tp = 10 s.

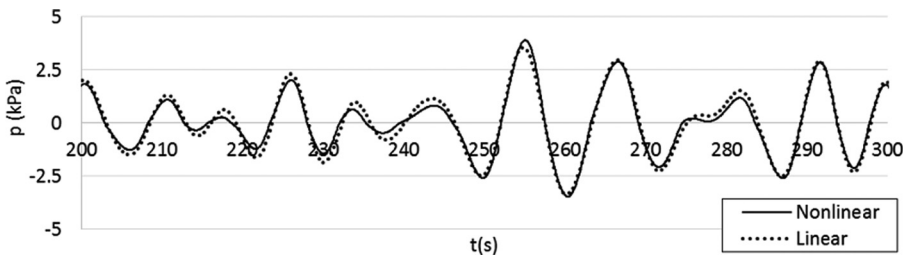

FIG. 25. Chamber pressures for linear and nonlinear PTOs: Hs = 2 m and Tp = 10 s (fixed).

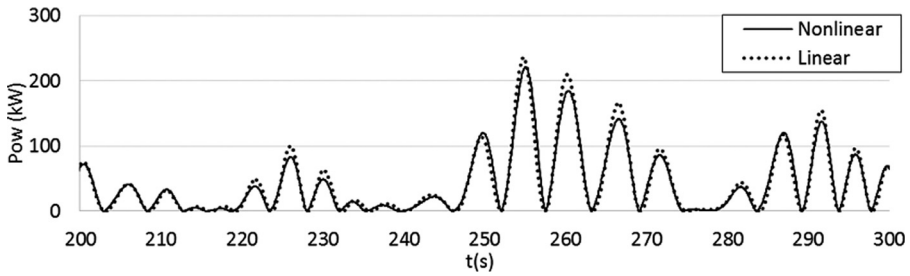

FIG. 26. Capture powers for linear and nonlinear PTOs: Hs = 2 m and Tp = 10 s (fixed).

The IWS responses can be seen in Figure 28, where a comparison of the responses of the IWS motions with and without additional damping is done. The additional damping reduces the response of the IWS motion so to make it reasonable in amplitude ($B_{99} = 40$ kN/(m/s)).

As shown in Eq. (40), for a fixed OWC, the air compressibility induces an increase in the spring coefficient for the internal water surface motion, and the IWS resonance period will be reduced accordingly (see Figures 29–32) (for all the cases, the PTO damping has been set as $K_1 = 28.04$ kN/(m/s)). This is different from those in the floating OWC, where the combined IWS motion can have a longer resonance period (see Figure 8(b)) due to the interactions between the device and the water body.

Similar to the floating OWC, the air compressibility has increased with the increase of volumetric ratio. For a large volumetric ratio of 5.0, the significant difference of the responses can be seen for the cases with and without air compressibility.

The effects of the air compressibility on the maximal capture power in irregular waves are shown in Figure 32. For longer waves (Tp > 10 s), air compressibility reduces the power captured from the irregular waves, and the larger the air compressibility, the larger reduction can be seen. However, it can also show a small increase for the short waves in the cases of small air compressibility, and this can be understood as the result of the reduced resonance periods due to air compressibility. For the cases of very larger air compressibility, through the reduced resonance periods, the capture power is decreased due to the large air compressibility. This is again different from those in the floating OWC, where small air compressibility may increase the power conversion for all wave periods though the increase may only be marginal (see Figure 18).

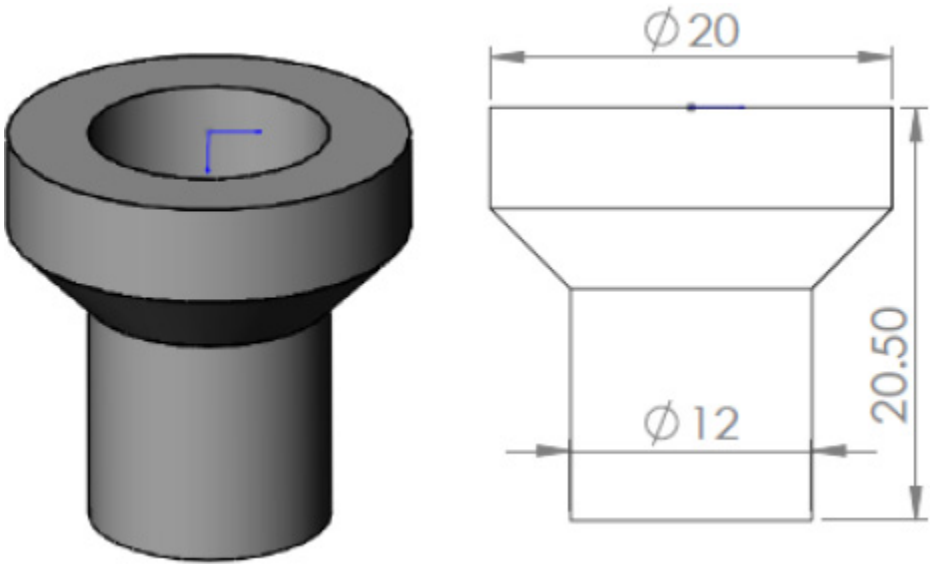

FIG. 27. Fixed OWC with a draft being adjusted to have a resonance period $T_0 = 10$ s, corresponding to the low resonance period of the floating OWC.

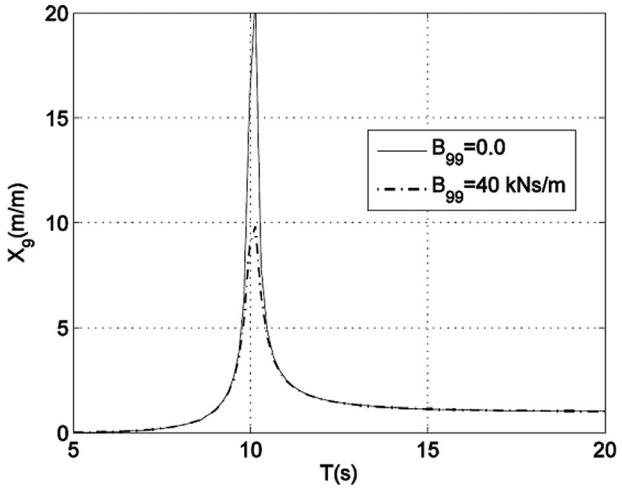

FIG. 28. Heave responses of water body in the fixed OWC with and without additional damping coefficients.

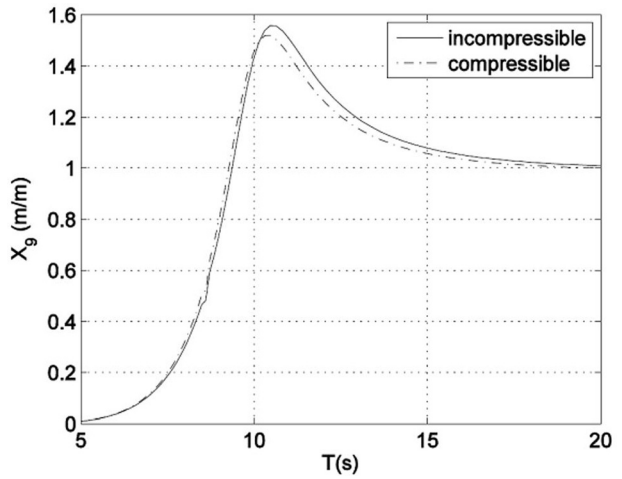

FIG. 29. Heave response comparison of the water body with and without air compressibility: Vr = 1.0.

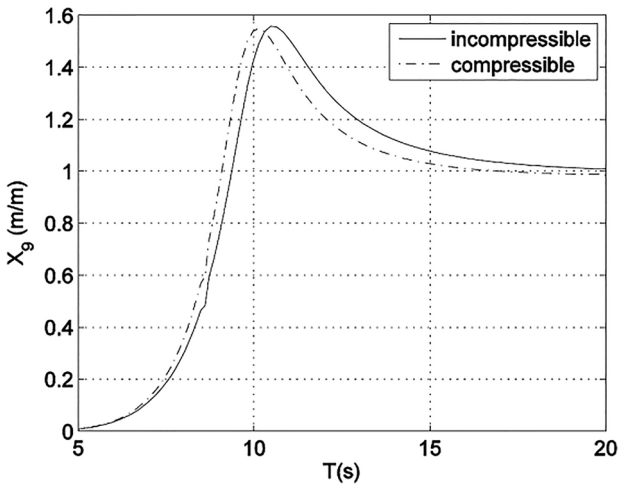

FIG. 30. Heave response comparison of the water body with and without air compressibility: Vr = 2.5.

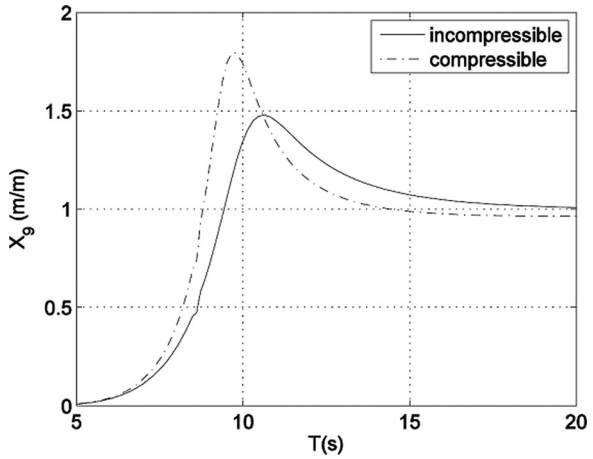

FIG. 31. Heave response comparison of the water body with and without air compressibility: Vr = 5.0.

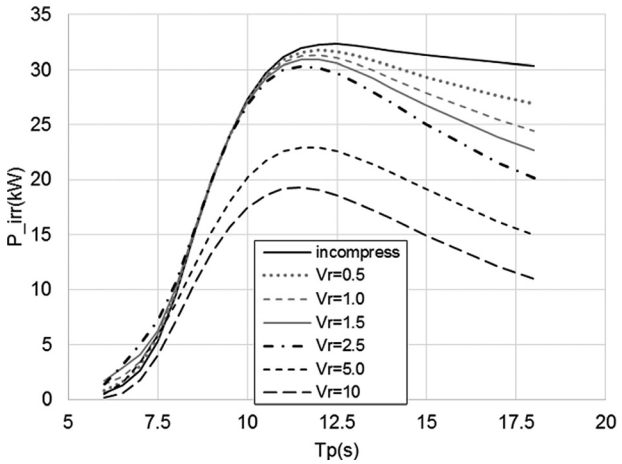

FIG. 32. Maximal capture power for different air volumes.

VII. CONCLUSIONS

The research work has been focused on the performance and power capture of the OWC wave energy converters, including the effect of air compressibility. From the development and the analysis, the following conclusions can be drawn:

– The formula for studying air compressibility for the OWC wave energy converters has been formulated in the frequency domain, and from which, air compressibility in the air chamber has been shown to contribute to both the increase of the self-spring term and decrease in the coupling spring term for the floating OWC, and for the fixed OWC, air compressibility invariably increases the spring coefficient for the water body.
– Due to air compressibility, the actual PTO damping coefficient is reduced due to air compressibility, and it is frequency-dependent even if a constant PTO damping coefficient is given.
– Small air compressibility may be good for marginally improving the OWC wave energy conversion performance, but large air compressibility may lead to significant reductions in the wave energy conversion for the floating OWC.
– For the fixed OWC, air compressibility will reduce the power conversion for long waves, and the reduction increases with the increase of air compressibility. However, small air compressibility may increase the capture power for short waves.

– The simplified PTO flowrate calculation made by Sarmento *et al.*[26] is a very good approximation in practical OWC devices, unless the wave heights become very large.
– Due to the existence of large air compressibility in the OWC air chamber, the chamber pressure with a nonlinear PTO may become smoother (i.e., more linear), whilst the flowrate through the PTO becomes nonlinear with transitions near the zeros.
– Regardless of the PTO types (linear or nonlinear) and of air compressibility, the flowrate driven by the IWS is generally linear.

ACKNOWLEDGMENTS

This material is based on the works supported by Science Foundation Ireland (SFI) under the Charles Parsons Award for Ocean Energy Research (Grant No. 06/CP/E003) in collaboration with MaREI, the SFI Centre for Marine Renewable Energy Research (Grant No. 12/RC/2302), Environment Research Institute, University College Cork, Ireland. Statistics and data were correct at the time of writing the article; however, the authors wish to disclaim any responsibility for any inaccuracies that may arise.

[1]G. Mork *et al.*, "Assessing the global wave energy potential," in Proceedings of OMAE2010 29th International Conference on Ocean, Offshore Mechanics and Arctic Engineering, Shanghai, China, 2010.
[2]D. Magagna and A. Uihleih, "Ocean energy development in Europe: Current status and future perspectives," Int. J. Mar. Energy **11**, 84–104 (2015).
[3]M. E. McCormick, *Ocean Wave Energy Conversion* (Dover Publications, Inc., 2007).
[4]A. Falcao, "Wave energy utilization: A review of the technologies," Renewable Sustainable Energy Rev. **14**(3), 899–918 (2010).
[5]See http://www.oceanpowertechnologies.com/ for OPT, Ocean power technologies; accessed 10 March 2015.
[6]Aquamarine, *Aquamarine Power*, 2013.
[7]T. Heath, "A review of oscillating water columns," Philos. Trans. R. Soc., A **370**, 235–245 (2012).
[8]R. Yemm *et al.*, "Pelamis: Experience from concept to connection," Philos. Trans. R. Soc., A **370**, 365–380 (2012).
[9]A. Pecher *et al.*, "Performance assessment of the pico OWC power plant following the equimar methodology," in Proceedings of the Twenty-first (2011) International Offshore and Polar Engineering Conference, Maui, Hawaii, USA, 2011.
[10]J. Tedd and J. Peter Kofoed, "Measurements of overtopping flow time series on the Wave Dragon, wave energy converter," Renewable Energy **34**(3), 711–717 (2009).
[11]See http://www.el.angstrom.uu.se/forskningsprojekt/WavePower/Lysekilsprojektet_E.html for Uppsala-University, Wave Power Project - Lysekil; accessed 25 October 2012.
[12]Y. Torre-Enciso *et al.*, "Mutriku Wave Power Plant: From the thinking out to the reality," in Proceedings of the 8th European Wave and Tidal Energy Conference, Uppsala, Sweden, 2009.
[13]J. Hals-Todashaug *et al.*, "Tank testing of an inherently phase controlled wave energy converter," in Proceedings of the 11th European Wave and Tidal Energy Conference, Nantes, France, 2015.
[14]P. Casaubieilh *et al.*, "Performance improvements of mooring systems for wave energy converters," in Proceedings of the 1st Renewable Energies Offshore, RENEW 2014, Lisbon, Portugal, 2014.
[15]W. Sheng, R. Alcorn, and A. Lewis, "Assessment of primary wave energy conversions of oscillating water columns. I. Hydrodynamic analysis," J. Renewable Sustainable Eng. **6**, 053113 (2014).
[16]W. Sheng, R. Alcorn, and A. W. Lewis, "Assessment of primary wave energy conversions of oscillating water columns. II. Power take-off and validations," J. Renewable Sustainable Energy **6**, 053114 (2014).
[17]A. Falcao and J. C. C. Henriques, "Oscillating water column wave energy converters and air turbines: A review," Renewable Energy **85**, 1391–1424 (2016).
[18]D. V. Evans and R. Porter, "Hydrodynamic characteristics of an oscillating water column device," Appl. Ocean Res. **17**(3), 155–164 (1995).
[19]A. J. N. A. Sarmento and A. F. D. O. Falcao, "Wave generation by an oscillating surface pressure and its application in wave-energy extraction," J. Fluid Mech. **150**, 467–485 (1985).
[20]D. V. Evans, "Wave-power absorption by systems of oscillating surface pressure distributions," J. Fluid Mech. **114**, 481–499 (1982).
[21]M. Alves *et al.*, "Performance evaluation of an axisymmetric floating OWC," in The Proceedings of the 12th (2010) International Offshore and Polar Engineering Conference, Beijing, China, 2010.
[22]A. Falcao, J. C. C. Henriques, and J. J. Candido, "Dynamic and optimization of the OWC spar buoy wave energy converter," Renewable Energy **48**, 369–381 (2012).
[23]S. Nagata *et al.*, "Frequency domain analysis on primary conversion efficiency of a floating OWC-type wave energy converter 'Backward bent Duct Buoy'," in Proceedings of the 9th European Wave and Tidal Energy Conference, Southampton, UK, 2011.
[24]W. Sheng, A. W. Lewis, and R. Alcorn, "Numerical studies of a floating cylindrical OWC WEC," in Proceedings of the ASME 2012 31st International Conference on Ocean, Offshore and Arctic Engineering, OMAE 2012, Rio de Janeiro, Brazil, 2012.
[25]A. F. d. O. Falcao and P. A. P. Justino, "OWC wave energy devices with air flow control," Ocean Eng. **26**(12), 1275–1295 (1999).
[26]A. J. N. A. Sarmento, L. M. C. Gato, and A. F. de O. Falcao, "Turbine-controlled wave energy absorption by oscillating water column devices," Ocean Eng. **17**(5), 481–497 (1990).

[27]W. Sheng, R. Alcorn, and A. Lewis, "On thermodynamics of primary energy conversion of OWC wave energy converters," J. Renewable Sustainable Eng. **5**, 023105 (2013).
[28]A. Thakker *et al*., "Effects of compressibility on the performance of a wave-energy conversion device with an impulse turbine using a numerical simulation technique," Int. J. Rotating Mach. **9**, 443–450 (2003).
[29]C. Josset and A. H. Clement, "A time-domain numerical simulator for oscillating water column wave power plants," Renewable Energy **32**(8), 1379–1402 (2007).
[30]A. Brito-Melo, L. M. C. Gato, and A. J. N. A. Sarmento, "Analysis of Wells turbine design parameters by numerical simulation of the OWC performance," Ocean Eng. **29**(12), 1463–1477 (2002).
[31]J. Weber, "Representation of non-linear aero-thermodynamics effects during small scale physical modelling of OWC WECs," in Proceedings of the 7th European Wave and Tidal Energy Conference, Porto, Portugal, 2007.
[32]W. Sheng, R. Alcorn, and A. Lewis, "Physical modelling of wave energy converters," Ocean Eng. **84**, 29–36 (2014).
[33]A. Falcao and J. C. C. Henriques, "Model-prototype similarity of oscillating-water column wave energy converters," Int. J. Mar. Energy **6**, 18–34 (2014).
[34]W. Sheng and A. Lewis, "Power take-off optimisation for maximising energy conversion of wave activated bodies," IEEE J. Oceanic Eng. **41**, 529–540 (2016).
[35]R. Taghipour, T. Perez, and T. Moan, "Hybrid frequency-time domain models for dynamic response analysis of marine structures," Ocean Eng. **35**(7), 685–705 (2008).
[36]W. Sheng, R. Alcorn, and A. Lewis, "A new method for radiation forces for floating platforms in waves," Ocean Eng. **105**, 43–53 (2015).
[37]G. Duclos, A. H. Clement, and G. Chatry, "Absorption of outgoing waves in a numerical wave tank using a self-adaptive boundary condition," Int. J. Offshore Polar Eng. **11**(2), 168–175 (2001).
[38]W. Sheng and A. Lewis, "Assessment of wave energy extraction from seas: Numerical validation," J. Energy Resour. Technol. **134**, 041701 (2012).
[39]R. P. F. Gomes *et al*., "Hydrodynamic optimisation of an axisymmetric floating oscillating water column for wave energy conversion," Renewable Energy **44**, 328–339 (2012).
[40]W. Sheng and A. Lewis, "Power take-off optimisation to maximise wave energy conversions for oscillating water column devices," J. Oceanic Eng. (revision, unpublished).